Novel sst_5-Selective Somatostatin Dicarba-Analogues: Synthesis and Conformation−Affinity Relationships

Debora D'Addona,[†] Alfonso Carotenuto,*[,‡] Ettore Novellino,[‡] Véronique Piccand,[§] Jean Claude Reubi,[§] Alessandra Di Cianni,[†] Francesca Gori,[△] Anna Maria Papini,[†] and Mauro Ginanneschi*[,†]

Laboratory of Peptides and Proteins, Chemistry and Biology, Department of Organic Chemistry, University of Firenze, Via Lastruccia 13 I-50019, Sesto Fiorentino, Italy, Department of Pharmaceutical Chemistry and Toxicology, University of Napoli, Via Domenico Montesano 49, Italy, Division of Cell Biology and Experimental Cancer Research, Institute of Pathology, University of Berne, Murtenstrasse 31 CH-3010 Berne, Switzerland, and Laboratory of Peptides and Proteins, Chemistry and Biology, Department of Pharmaceutical Sciences, University of Firenze, Via U. Schiff 6 I-50019, Sesto Fiorentino, Italy

Received July 24, 2007

We describe synthesis, conformational studies, and binding to the five somatostatin receptors (sst_{1-5}) of a few analogues of the cyclic octapeptide octreotide (**1**), where the disulfide bridge was replaced by a dicarba group. These analogues were prepared by on-resin RCM of linear hepta-peptides containing two allylglycine residues; first- and second-generation Grubbs catalyst efficiencies were compared. The C═C bridge was hydrogenated via two different methods. Binding experiments showed that two analogues had good affinity and high selectivity for the sst_5 receptor. Three-dimensional structures of the active analogues were determined by ^{1}H NMR spectroscopy. Conformation−affinity relationships confirmed the importance of D-Phe^2 orientation for sst_2 affinity. Moreover, helical propensities well correlates with the peptide sst_5 affinity. The presence of the bulky aromatic side chain of Tyr(Bzl)^{10} favored the formation of a 3_{10}-helix and enhanced the sst_5 selectivity suppressing the sst_2 affinity. Finally, a new pharmacophore model for the sst_5 was developed.

Introduction

The highly potent cyclic peptide somatostatin (SRIF[a]; H-Ala^1-Gly^2-*c*[Cys^3-Lys^4-Asn^5-Phe^6-Phe^7-Trp^8-Lys^9-Thr^{10}-Phe^{11}-Thr^{12}-Ser^{13}-Cys^{14}]-OH, SRIF-14) was isolated from mammalian hypothalamus[1] and first synthesized by J. Rivier.[2] Later on, it was found that native SRIF occurs in two biologically active forms, SRIF-14 and a 28-residue peptide, SRIF-28.[3] The natural hormone is widely distributed in the endocrine and central nervous systems and it has many modulating actions in the body, such as growth hormone (GH) inhibition, glucacon, insulin, and gastrin release suppression. A family of five G-protein-coupled somatostatin receptors (sst_{1-5}) located in the cell membrane mediates the biological effects of SRIF.[4] The individual signaling pathway of each SRIF receptor is still not completely clarified,[4] being complicated by transmembrane domain interactions. It is known that some of these receptors, mainly the sst_2 and sst_5 subtypes, mediate the antiproliferative effects of SRIF on cellular growth of many sort of tumors. The clinical use of native SRIF has been precluded by its short half-life in vivo (1–2 min) but the broad spectrum of physiological activity of this hormone has prompted many researchers to investigate the structural requirements necessary to elicit the biological activity. As a consequence, in the past decades, hundreds of peptide and nonpeptide analogues were synthesized and tested for their structure–activity relationships.[5] Among them, octreotide (**1**) (Figure 1; Sandostatin, SMS 201-995), a cyclic octapeptide SRIF agonist, was synthesized by Sandoz researchers.[6] It showed high affinity and specificity toward sst_2 receptor subtype.[4] However, the administration of **1** itself as a cell growth inhibitor was successful only in a few cancer types as acromegaly and metastatic carcinoid diseases.[7] It is used in clinical protocols mainly as a carrier of radionuclides for diagnostic or therapeutic purposes.[4,8,9]

Peptide **1** incorporates D-Trp in place of Trp^8 of SRIF and exhibits the so-called pharmacophore sequence, Phe^7-D-Trp^8-Lys^9-Thr^{10} (Note: numbering of the residues follows that of native SRIF). The disulfide tether of **1** (Figure 1) stabilizes a β-turn structure spanning the D-Trp^8-Lys^9 residues, supposed to be mandatory for the binding to the ssts.[10] On the other hand, it is well-known that the disulfide bridge is prone to be attacked by endogenous reducing enzymes or by nucleophilic and basic agents.[11] Furthermore, the labeling of the octreotide derivatives with isotopes such as ^{99m}Tc and ^{188}Re needs a step in reducing *medium* that can afford ring cleavage, especially at the level of the disulfide linkage.[9] The search for more robust octreotide derivatives, carrying a stable bridging tether, prompted us to consider the dicarba-analogues as a convenient target. In the past, Veber and co-workers prepared nonreducible derivatives of SRIF by using aminosuberic or diaminosuberic acid as building blocks in the peptide chain synthesis.[12,13] Similarly,

* To whom correspondence to be addressed. Phone: +39-081-678626(A.C.); +39-055-4573525 (M.G.). Fax: +39-081-678644 (A.C.); +39 055 4573531 (M.G.). E-mail: alfonso.carotenuto@unina.it (A.C.); mauro.ginanneschi@unifi.it (M.G.).

† Department of Organic Chemistry, University of Firenze.

‡ University of Napoli.

§ University of Berne.

△ Department of Pharmaceutical Sciences, University of Firenze.

[a]Abbreviations: Bzl, benzyl; dhDsa-C, dehydrodiaminosuberic acid C-terminus; dhDsa-N, dehydrodiaminosuberic acid N-terminus; Dsa-C, diaminosuberic acid C-terminus; Dsa-N, diaminosuberic acid N-terminus; DMF, *N*,*N*-dimethylformamide; DMSO-d_6, hexadeuteriodimethylsulfoxide; DOTA, tetraazacyclododecanetetraacetic acid; DQF-COSY, double quantum filtered-correlation spectroscopy; DTPA, diethylene-tetraaminepentaacetic acid; EDT, 1,2-ethanedithiol; ESI-MS, electrospray ionization mass spectrometry; Fmoc, 9-fluorenylmethoxycarbonyl; GH, growth hormone; Hag, L-2-allyl-Gly; HATU, hexafluorophosphate salt of the *O*-(7-azabenzotriazol-yl)-tetramethyl uranium cation (this acronym no longer corresponds to the true structure); MD, molecular dynamics; NMM, *N*-methyl morpholine; NOE, nuclear Overhauser effect; NOESY, nuclear Overhauser enhanced spectroscopy; PE COSY, primitive exclusive correlated spectroscopy; RCM, ring-closing metathesis; RMSD, root mean square deviation; RP-HPLC, reverse phase high performance liquid chromatography; SPE, solid phase extraction; SPPS, solid phase peptide synthesis; SRIF, somatostatin; sst, somatostatin receptor; TFA, trifluoroacetic acid; TOCSY, total correlated spectroscopy; TSP, 3-trimethylsilanylpropionic acid.

10.1021/jm070886i CCC: $40.75
Published on Web 01/23/2008

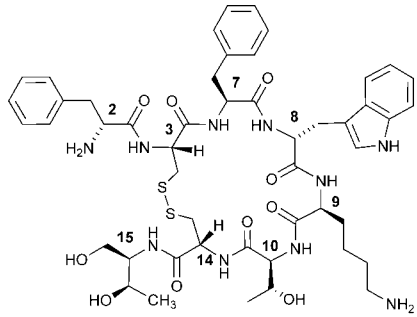

1

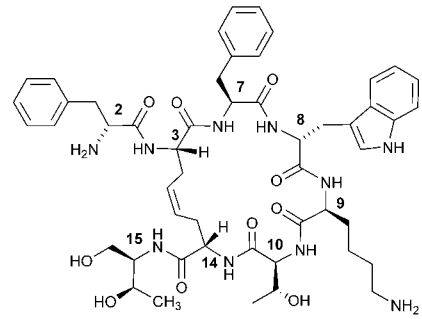

2

Figure 1. Structures of **1** and of dicarba SRIF mimetic (**2**).

Table 1. Peptide Sequences; General Formula: D-Phe^2-*c*[Xaa^3-Phe^7-D-Trp^8-Lys^9-Yaa^{10}-Zaa^{14}]-Thr(ol)^{15}-OH

peptide	Xaa	Yaa	Zaa
1	Cys	Thr	Cys
2	dhDsa-N	Thr	dhDsa-C
11	dhDsa-N	Tyr(Bzl)	dhDsa-C
12	dhDsa-N	Phe	dhDsa-C
13	Dsa-N	Thr	Dsa-C[d]
14	Dsa-N	Tyr(Bzl)	Dsa-C

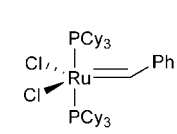

3

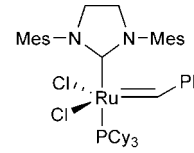

4

Figure 2. First-generation (**3**) and second-generation Grubbs catalyst (**4**).

Gilon's group has recently prepared constrained backbone-cyclic analogues with high conformational stability by cyclization through synthetic C_α bifunctional aminoacids.[14,15] The discovery of the olefin metathesis reaction disclosed the way for synthesis and cleavage of carbon−carbon bonds under mild conditions.[16] In particular, the use of ring-closing metathesis (RCM) reactions catalyzed by ruthenium complexes has become a popular method for the formation of C═C bridged structures in organic syntheses.[17] Application of this method to amino acids bearing unsaturated side chains (i.e., allylglycine) and located in strategic positions of the peptide motif allows the preparation of carba-cyclic peptides by the SPPS method.[18–21] Moreover, it is known that constrained carba-tethers in cyclic peptides can stabilize helices or β-turns.[22,23] However, the effect of the change of the dihedral angle of disulphide bridge on receptors affinity of these synthetic peptides is not easily predictable.[18]

We first applied RCM to the on-resin cyclization of D-Phe^2-Hag^3-Phe^7-D-Trp^8-Lys^9-Thr^{10}-Hag^{14}-Thr(ol)^{15}, obtaining the analogue **2** (Figure 1, and Table 1). This compound is stable in the enzymatic pool of the human serum for more than 30 h. NMR analysis in aqueous solution followed by restrained MD simulations showed that the peptide has a conformational behavior very similar to that of the parent peptide **1**.[24] In the present work we have resynthesized compound **2** with an improved synthetic strategy, and we have also prepared the corresponding reduced analogue **13**, containing the more flexible CH_2-CH_2 tether (Table 1).

Almost at the same time, another group published the synthesis of dicarba-analogues of **1**, lanreotide, and vapreotide and their hydrogenation products.[25] However, no data on the conformations of these compounds or on their ability to bind with sst receptors were reported by these authors.

Apart from peptides **2** and **13**, in the present paper new analogues have been developed. Recent studies on the structure–activity relationships of sst ligands, which have called attention to the role of lipophilic residues (Phe^{6,7,11}) of the native hormone[26] prompted us to prepare new synthetic dicarba-analogues by substituting Thr^{10} residue with Tyr(Bzl) (Bzl = benzyl) and Phe (compounds **11** and **12**, respectively, Table 1). To aim this, we exploited a new solid phase support, modifying the synthetic pathway and comparing the efficiency of the first and second generation Grubbs catalysts (namely, structures **3** and **4**, respectively; Figure 2).

The ethylene group of the analogue **11** was hydrogenated, affording the saturated derivatives **14** (Table 1). All the synthesized analogues were tested for the binding to the sst_{1-5} receptor subtypes. Herewith, we also suggest correlations between the binding data and the results of the conformational analysis carried out on these compounds via NMR and MD studies.

Results and Discussion

Peptide Synthesis and Purification. In our previous work,[24] the synthesis of the linear precursor of the analogue **2** started by anchoring the building block Fmoc-threoninol *p*-carboxybenzaldehyde acetal linker to the Rink amide resin.[27]The synthesis of this substance was complicated by the presence of an unidentified impurity, not detected by the preceding authors and difficult to remove. Moreover, for reducing the high substitution level of the Rink amide resin (1 mmol/g) to reach the pseudodilution conditions necessary to the cyclization step, we end-capped the free NH_2 groups with a $(CH_3CO)_2O$/CH_3COOH mixture. The following washing of the residual acetic acid, which is harmful for catalyst **3**, was a really time-consuming step. In the method here reported we used the H-L-Thr(*t*-Bu)-ol-2-chlorotrityl resin which already contains the [Thr(ol)^{15}] of the sequence (Scheme 1).

After the coupling of the Fmoc-Hag^3, the resin loading (0.5 mmol/g) already met the requirements of the pseudodilution effect, minimizing the risk of the formation of intermolecular bonds. However, the RCM with catalyst **3** of the linear octapeptide precursors linked to the Rink amide resin as well as to the trityl resin gave unsatisfactory yield of the cyclic compounds **2** and **11** and only traces of **12** (Supporting Information). The factors that affect the success of the RCM on peptide cyclization are not yet fully understood. Probably inappropriate orientation of the alkenyl side chains may hamper the RCM. In general, the solid-phase RCM was carried out on peptides containing proline or *N*-alkyl residues in the sequence[28] and only recently dicarba-analogues of oxytocin were prepared by RCM on solid phase of the parent linear peptides.[20,21]

Scheme 1. Synthesis of Linear Peptides[a]

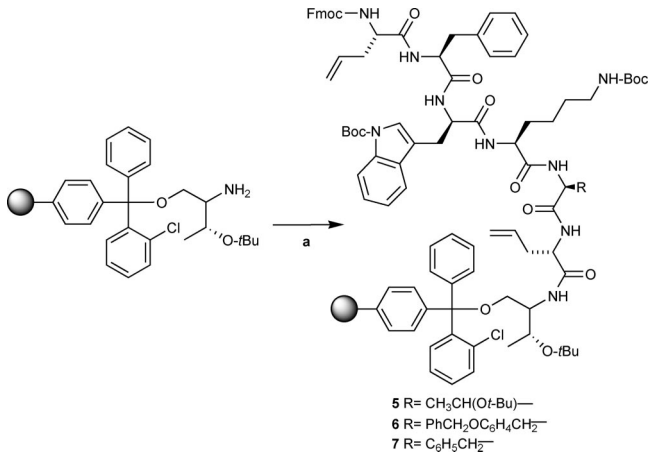

[a] Reagents and conditions: (a) (i) Fmoc-Hag, HATU/NMM, 50 min, rt; (ii) 20% piperidine in DMF (2 × 15 min); (iii) coupling with the following amino acids: Fmoc-L-Thr(*t*-Bu) (**5**), Fmoc-L-Tyr(Bzl) (**6**), Fmoc-L-Phe (**7**), Fmoc-L-Lys(Boc), Fmoc-D-Trp(Boc), Fmoc-L-Phe; Fmoc-Hag.

Consequently, we planned a more convenient synthetic approach to these cyclopeptides. The elongation of the peptide sequence was stopped after the coupling of Hag[3] residue (Scheme 1), with the aim of removing any possible interference of the aromatic ring of D-Phe on the correct orientation of the allylglycine side chains. The linear hepta-peptides **5**–**7** were then converted by RCM with catalyst **3** to the corresponding cyclic analogues **8**–**10** (Scheme 2).

The D-Phe[2] terminal residue was added only after the cyclization step (Scheme 2), affording the analogues **2** and **11** in an amount suitable for the next physicochemical and biological studies. In the case of **12**, due to the still persisting poor linear-to-cyclic conversion, we were able to isolate the cyclic peptide only for characterization purposes. A new generation Grubbs catalysts, like 1,3-dimesitylimidazol-2-ylidene **4** (Figure 2), was considered. The second generation showed higher stability than the phosphine analogue **3**, less sensibility to nucleophilic groups present in the molecule, and was more active in most metathesis reactions.[29,30] Comparison between the efficiency of catalysts **3** and **4** on the RCM reaction of the acyclic heptapeptides **5**−**7** is reported in Table 2. Catalyst **4** increased the yield by 10% and shortened the reaction time for all peptide sequences. It is worth noting that the presence of Phe[10] negatively affected the RCM no matter what kind of catalyst was used. The Phe residue close to Hag[14] hampered the RCM more than the bulky aromatic Tyr(Bzl)[10]. This suggests that RCM is not affected by the size of the residue in position 10 but probably by the influence it has on the proper orientation of the allyl side chains of Hag[3] and Hag[14]. In both reaction conditions (catalysts **3** and **4**), no significant dimerization or oligomerization byproduct was observed by HPLC-ESI inspection.

The cleavage of the cyclopeptide **11** from the resin required a more diluted TFA solution than for **2** and **12** to prevent the contemporary hydrolysis of the Bzl group. The isolation of peptides obtained on-resin by RCM is often complicated by the tendency of the organometallic molecules to bind the solid support. Several washing methods have been suggested to eliminate Ru contaminants.[21,31–33] However, not one of them gave satisfactory results in our hands. Notably, we found that repeated treatments of the resin with fresh piperidine solutions before the coupling with Fmoc-D-Phe, centrifugation of the aqueous suspension after the cleavage and separation by SPE, if necessary, afforded compounds that were then easily purified

Scheme 2. Synthesis of Cyclic Peptides (**2**, **11**, **12**)[a]

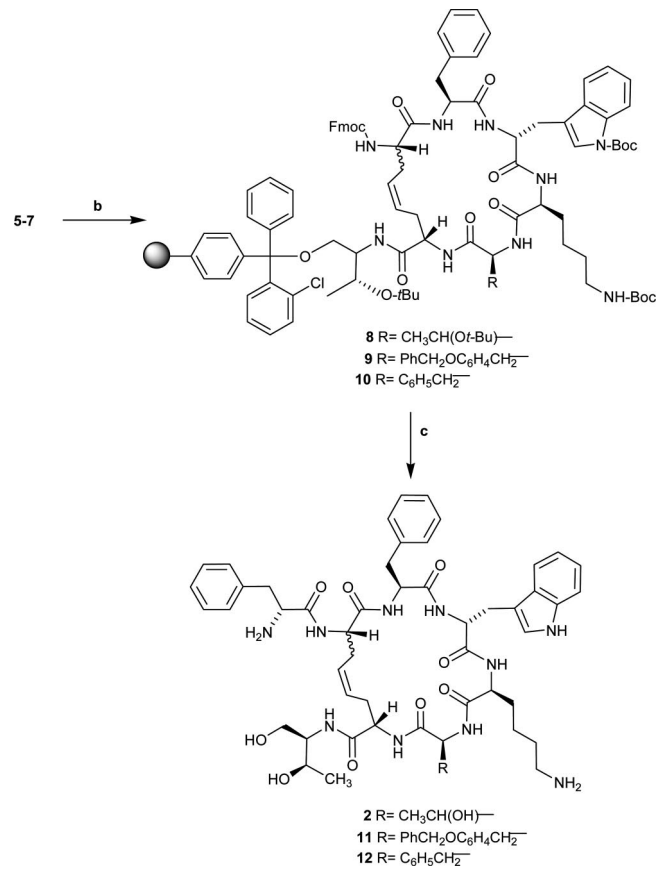

[a] Reagents and conditions: (b) catalyst 3, 40 °C, 48 h (**8**, **9**) or 52 h (**10**); catalyst 4, 40 °C, 24 h (**8**, **9**) or 48 h (**10**); (c) (i) 20% piperidine in DMF, Fmoc-D-Phe/HATU/NMM 50 min, rt; (ii) 20% piperidine in DMF; cleavage of **2** and **12** [TFA/H_2O/EDT/phenol (94:2:2:2)]; **11** [TFA/H_2O/EDT/phenol (70:26:2:2)].

Table 2. Cyclization of the Linear Hepta-Peptides **5**, **6**, and **7** with catalyst 3 or 4

dicarba-analogues	catalyst (hours of reflux)	% yield[a]	cyclic/linear ratio[b]
2	**3** (48)	25	85:15
2	**4** (24)	35	90:10
11	**3** (52)	10	50:50
11	**4** (48)	20	80:20
12	**3** (48)	3	30:70
12	**4** (24)	13	50:50

[a] Overall yield of isolated pure compounds, calculated on the basis of an average peptide loading of 0.5 mmol/g of resin. [b] Calculated on the basis of peak area in analytical RP-HPLC.

from the residual catalyst contaminants by semipreparative HPLC. Compounds **2** and **11** obtained by RCM with catalyst **4** were directly purified by RP-HPLC due to the low level of contaminants. Finally, analytical RP-HPLC and ESI-MS analysis of the crude compounds **2**, **11**, and **12** showed two chromatographic peaks with the same MW, probably corresponding to geometric isomers (ratio ≈ 90:10). In any case, binding and conformational studies were performed only on the most abundant isomer. The olefinic bridge of the analogues **2** and **11** was hydrogenated to study the effect of the higher flexibility of the $-CH_2-CH_2-$ group on the conformational behavior. Low yield of peptide **12** prevented us from preparing its hydrogenated derivative. Hydrogenation of **2** and **11** was accomplished using two different methods because of the different substitution in position 10. The Pd/C catalyst, which is the most used tool to reduce olefinic bridges obtained by RCM

Scheme 3. Synthesis of Saturated Analogues **13** and **14**[a]

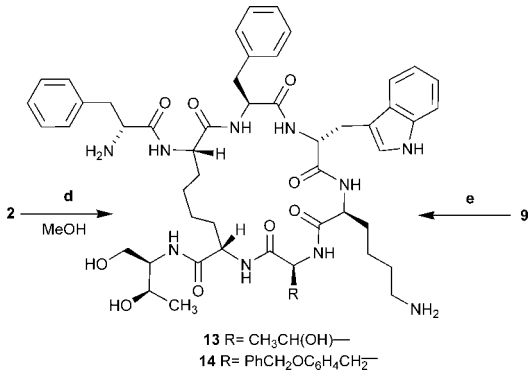

[a] Reagents and conditions: (d) 20% $Pd(OH)_2/C$, H_2, 24 h, 30 °C; (e) (i) MeOH/DCM, Wilkinson's catalyst 2.5%, H_2 (60 psi); (ii) 20% piperidine in DMF, Fmoc-D-Phe/HATU/NMM, 50 min, rt; (iii) 20% piperidine in DMF, cleavage.

on peptides, did not work well for the reduction of **2**. Therefore, the saturated analogue **13** was obtained by using H_2 fluxing in the presence of $Pd(OH)_2/C$. However, heating at 30 °C of the reaction mixture was needed to obtain compound **13** in good yields (Scheme 3).

The analogue **14**, obtained from the parent **11** (Table 1), was achieved by using Wilkinson's catalyst,[34,35] to prevent the cleavage of the Bzl group by the palladium catalyst (Scheme 3).

Binding Affinity to sst_{1-5} Receptors. All compounds were tested for their ability to bind to the five human sst_{1-5} receptor subtypes in complete displacement experiments using the universal SRIF radioligand [^{125}I]-[Leu^8,D-Trp^{22},Tyr^{25}]-SRIF-28. SRIF-28 was run in parallel as control. IC_{50} values were calculated after quantification of the data using a computer-assisted image processing system. The data are shown in Table 3. Binding data (Table 3) indicate that **2** shows nM binding affinities toward the sst_2, sst_4, and sst_5.

Compared to the parent peptide **1**,[5] the affinities toward sst_2 and sst_5 receptors were reduced (about 20-fold for sst_2 and about 5-fold for sst_5) and the affinity toward sst_3 receptor was abolished. Peptide **13** shows similar binding affinity profiles toward the ssts compared to that of **2**. The affinity toward sst_5 significantly decreased (203 vs 28 nM, Table 3). Compound **12** shows only low affinity toward $sst_{4/5}$. Therefore, we did not undertake the scale-up of the synthesis to provide the starting material for the double bond hydrogenation.

Most interestingly, binding data indicate that **11** is a ligand less potent than SRIF (IC_{50} = 29 nM) but by far more selective (at least 30-fold) for the sst_5 subtype (Table 3). Peptide **14** shows an enhanced affinity toward the sst_5 compared to **11** (IC_{50} = 12 nM), while its selectivity appears only slightly reduced (Table 3).

Not many selective sst_5 ligands have been found until now. Gilon et al. developed a backbone-cyclic sst (PTR 3046) with high selectivity toward sst_5.[36] The IC_{50} value for the binding of PTR 3046 to sst_5 was 67 nM, more than double compared to our compounds **11** and **14**. Some sst_5-selective nonpeptide peptidomimetics have been also reported. One of them, named L-817,818 with some selectivity to sst_5 has been obtained at the Merck laboratories through combinatorial chemistry approach.[37] L-817,818 showed sub-nM affinity toward sst_5 (IC_{50} = 0.4 nM), but it was only 8-fold more selective for sst_5 as compared to sst_1. The synthesis and screening of a focused library of β-turn mimetics based upon the crucial Trp-Lys motif, found in the turn region of SRIF, resulted in the identification of a small molecule ligand selective toward sst_5.[38] Its affinity toward sst_5 (IC_{50} = 87 nM) was lower compared to our selective compounds. Finally, two highly potent sst_4/sst_5 peptidomimetics have been recently described by Feytens et al.[39] Their structure is based on a constrained tryptophan scaffold, and the most potent analogue has an IC_{50} value of 1.2 nM for the sst_5. These compounds showed also high affinity toward sst_4 being only 3- and 9-fold more selective for sst_5 as compared to sst_4.

Hence, peptides **11** and **14** are among the most potent and sst_5-selective compounds reported to date. The potential therapeutic utility of selective agonists for sst_5, which is expressed in the lymphoid system, in pancreatic beta cells, and in corticotroph adenoma cells has been reported.[4]

NMR Analysis. NMR analysis of the analogues **2**, **11**, **13**, and **14**, was performed using 1D and 2D proton homonuclear experiments. NMR analysis of compound **12** was prevented by the low yield of this peptide. NMR experiments were recorded on a Varian Inova-Unity 700 MHz spectrometer in water/DMSO-d_6 8:2 solution (277.1 K) at 2 mM concentration. Solvent mixture was chosen since it allowed a better dispersion of the amide proton signals of some of the studied peptides compared to the water solution.

NMR Analysis of 13. Compound **13** is a carbocyclic analogue of **1**, with the disulfide group replaced by a CH_2-CH_2 bridge (Scheme 3). A qualitative analysis of short- and medium-range NOEs, $^3J_{NH-H\alpha}$ coupling constants, and temperature coefficients for exchanging NH was used to characterize the secondary structure of **13** (Supporting Information). Spectra analysis supported the presence of a β-turn about residues 3–6. Interestingly, the upfield shift observed for Hγs of Lys^9 (δ = 0.51, and δ = 0.30 ppm) has been used for decades as diagnostic for biological activity.[40,41]

Surprisingly, hydroxyl proton signal of Thr^{10}, which usually exchanges too quickly to be observed in water solution, was detected in the NMR spectra of **13**. This feature indicates that it can be engaged in a H-bond. NMR-derived constraints obtained for **13** were used as the input data for a simulated annealing structure calculation, as implemented within the standard protocol of the DYANA program.[42] NOEs were translated into interprotonic distances and used as upper limit constraints in subsequent annealing procedures to produce 200 conformations from which 50 structures were chosen, whose interprotonic distances best fitted NOE-derived distances and then refined through successive steps of restrained and unrestrained energy minimization calculations using the program Discover (Biosym, San Diego). A family of 20 structures, satisfying the NMR-derived constraints (violations smaller than 0.40 Å), was chosen for further analysis. The PROMOTIF program was used to extract details of the location and types of structural secondary motifs.[43] Backbone arrangement of **13** was well-defined, possessing an average root mean square deviation (rmsd) of the heavy atoms equal to 0.32 Å (Figure 3a).

The analysis of the secondary structure showed the existence of a distorted type II′ β-turn conformation about residues Phe^7-D-Trp^8-Lys^9-Thr^{10}. The turn structure is stabilized by hydrogen bonds between Phe^7 CO and Thr^{10} NH and between Phe^7 CO and Thr^{10} OH. The turn is flanked by two short, extended regions defining an antiparallel β-sheet. Also, the side chains have defined orientations (rmsd of all the heavy atoms equal to 0.88 Å). These orientations allowed a close spatial proximity between D-Phe^2-Dsa-N^3, Phe^7-Thr^{10}, and D-Trp^8-Lys^9 side chains. Finally, the sequential Thr^{10} NH-Dsa-C^{14}NH and Dsa-C^{14}NH-Thr(ol)^{15} NH NOEs, indicative of folded structures, are

Table 3. Receptor Affinities of the Somatostatin Analogues

	IC_{50}[a] (nM)				
No.	sst_1	sst_2	sst_3	sst_4	sst_5
SRIF-28	2.3 ± 0.4 (7)	3.0 ± 0.2 (7)	3.6 ± 0.5 (7)	1.6 ± 0.3 (7)	2.1 ± 0.2 (7)
2	>1000 (2)	44 ± 1 (2)	>1000 (2)	412 ± 68 (2)	28 ± 2 (2)
13	>1000 (2)	49 ± 12 (2)	>1000 (2)	214 ± 9 (2)	203 ± 106 (2)
12	961 ± 294 (2)	>1000 (2)	>1000 (2)	141 ± 27 (2)	206 ± 97 (2)
11	>1000 (2)	>1000 (2)	892 ± 245 (2)	>1000 (2)	29 ± 1 (2)
14	593 ± 39 (2)	393 ± 20 (2)	277 ± 123 (2)	846 ± 400 (2)	12 ± 2 (2)

[a] The number of independent repetitions to obtain the mean values ± SEM are indicated between brackets. SRIF-28 is used as internal control.

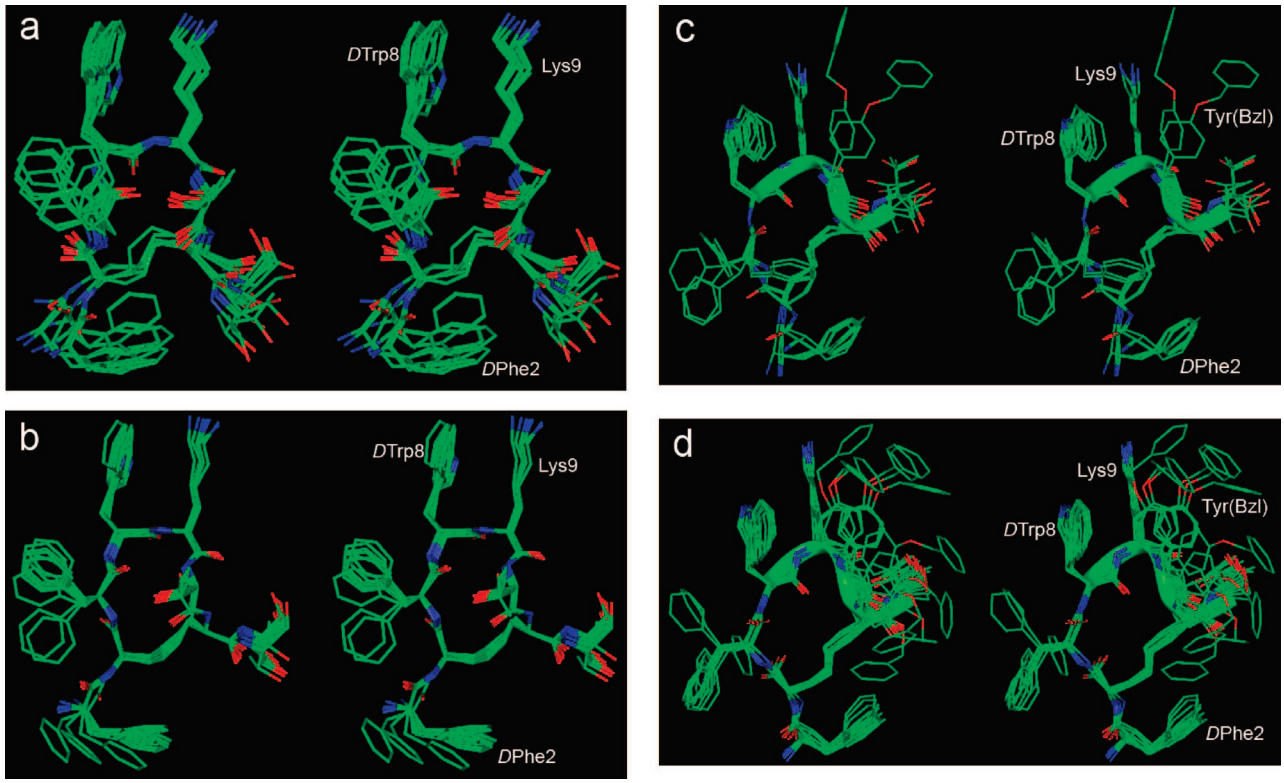

Figure 3. Stereoview of the 10 lowest-energy conformers of **13** (a), **2** (b), **14** (c), and **11** (d). Structures were superimposed using the backbone heavy atoms of residues 3–14. Heavy atoms are shown with different colors (carbon, green; nitrogen, blue; oxygen, red). Hydrogen atoms are not shown for clarity. C-terminal helical structure of compounds **14** and **11** was evidenced as a ribbon.

consistently violated by the β-sheet conformations (violations of about 0.30 Å). Melacini et al. found similar inconsistencies studying **1** in DMSO solution.[44] The authors hypothesized the existence of a conformational equilibrium between the β-sheet structural cluster and a second conformational ensemble involving folded structures for the C-terminal residues where the inconsistencies were observed. Therefore, a similar equilibrium should hold also for **13**. Superposition of the structure of **13** with that of **1**[44] (Protein Data Bank entry 1SOC) showed very similar structures in the active region (Figure 4). In contrast, the structure of the N-terminal D-Phe[2] and C-terminal Thr(ol)[15] residues are significantly different in the two peptides.

The distances between the Cγ atoms of the putative pharmacophoric side chains are reported in Table 4 together with those found by Melacini et al.[45] It can be observed that the distances found for **13** are in good accordance with the $sst_{2/3/5}$ pharmacophore.

NMR Analysis of 2. Compound **2** is the chemical precursor of **13**, with an unsaturated CH═CH bridge replacing the disulfide group of **1** (Scheme 2). In a recent paper, we have reported the NMR analysis of **2**.[24] The study showed that this peptide had a conformational behavior, in aqueous solution, very similar to the parent **1**. We reanalyzed the peptide in DMSO/

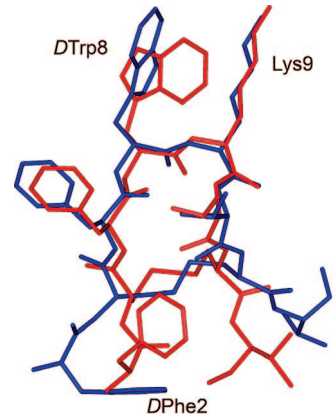

Figure 4. Superposition of the most representative structure of **13** (blue) with the structure of **1** (PDB entry 1SOC, red). Structures were superimposed using the backbone heavy atoms of residues 3–14. Hydrogen atoms are not shown for clarity.

H_2O solution at 277.1 K to compare its conformational behavior with the other analogues. A coupling constant value ($^3J_{CH=CH}$ = 8.1 Hz) between the two olefinic protons of the bridge and a relatively strong NOE between the same protons established

Table 4. Cγ−Cγ Distances (Å) between Putative Pharmacophoric Residues

cmpd	**13**	**14**	**11**	sst$_{2/3/5}$[a]
Ar^2-Ar^7	9.9 ± 0.5[b]	8.8 ± 0.5	9.5 ± 0.3	5–11
Ar^2-Ar^8	12.3 ± 0.5	12.2 ± 0.5	13.3 ± 0.2	11–15
Ar^2-Lys^9	13.4 ± 0.5	13.0 ± 0.6	14.3 ± 0.2	12–15
Ar^2-Ar^{10}		12.8 ± 0.5	12.6 ± 0.6	
Ar^7-Ar^8	7.2 ± 0.3	7.1 ± 0.5	7.3 ± 0.3	7–9
Ar^7-Lys^9	9.4 ± 0.2	10.1 ± 0.6	11.1 ± 0.3	9–11
Ar^8-Lys^9	4.8 ± 0.2	4.7 ± 0.4	4.9 ± 0.2	5
Ar^8-Ar^{10}		6.6 ± 0.5	7.3 ± 0.6	
Lys^9-Ar^{10}		4.8 ± 0.5	5.6 ± 0.6	

[a] Pharmacophore for the sst$_2$-, sst$_3$-, and sst$_5$-selective SRIF analogues.[45] [b] Average distance and standard deviation calculated from the ensemble of 10 structures.

the *Z*-geometry about the double bond. No signal attributable to the *E*-isomer could be detected in the spectra, indicating a unique configurational structure.

Compound **2** shows spectral features (Supporting Information) similar to those found in **13** but with some higher tendency to the helical structure. For instance, its NOESY spectra shows, at the same time, both strong Hα-9/NH-10, Hα-10/NH-14, and Hα-14/NH-15 NOE contacts, consistent with a β-sheet structural cluster and $d_{\alpha N}(i, i+2)$ diagnostic connectivities between Hα-8/NH-10, Hα-9/NH-14, and Hα-10/NH-15, characteristic of folded structures for the C-terminal residues. These data can be explained only hypothesizing an equilibrium between extended and folded conformational states, as already proposed for **1**.[44] Notably, calculated structures (Figure 3b) are characterized by an antiparallel β-pleated sheet with a type II′ β-turn at residues D-Trp^8/Lys^9, but several violations (NH-10/NH-14, Hα-10/NH-15, and NH-14/NH-15, Hβ-14/NH-15) were observed consistently with the hypothesized β-sheet/helical equilibrium.

NMR Analysis of 14. In compound **14**, as in **13**, the disulfide group of **1** is replaced by a CH_2-CH_2 bridge (Scheme 3). Compound **14** differs from **13** since Thr^{10} residue is replaced by the Tyr(Bzl) residue. Similar substitution into a cyclohexapeptide SRIF mimic led to the discovery of a potent sst$_{1-5}$ ligand.[26] NMR data (Supporting Information) clearly indicated the presence of a nascent helix or consecutive β-turn structures along residues 8–15. NMR-derived constraints obtained for **14** were used as the input data for a simulated annealing structure calculation, as described above.

The quality of the structure is reflected by the small rmsd (backbone heavy atoms rmsd = 0.48 Å), which can also be visually depicted from Figure 3c showing the bundle of 10 conformers representing the 3D structure.

From the backbone torsion angles, a distorted type II′ β-turn about residues D-Trp^8-Lys^9 followed by a short 3_{10}-helix along residues Tyr(Bzl)^{10}-Dsa-C^{14}-Thr(ol)^{15} can be identified (Figure 3c). The helical structure is stabilized by H-bonds between D-Trp^8 CO and Dsa-C^{14} NH and between Lys^9 CO and Thr(ol)^{15} NH. Helical structure is in conformational equilibrium with more extended conformations. In fact, violations of the NOE-derived distances Hα-9/NH-10, Hα-10/NH-14, and Hα-14/NH-15 (about 0.5 Å), together with relatively high temperature coefficients observed for NH-10, NH-14, and NH-15 ($-\Delta\delta/\Delta T > 3.0$ ppb/K, Supporting Information) indicate that the helical structure is quite flexible. Finally, side chains of D-Phe^2, Dsa-N^3, D-Trp^8, Lys^9, Tyr(Bzl)^{10}, and Dsa-C^{14} showed well-defined χ_1 values (i.e., *trans*, *gauche*$^+$, *trans*, *gauche*$^-$, *gauche*$^-$, and *gauche*$^-$ orientations, respectively). χ_1 values obtained by MD calculation are in accordance with the experimental $^3J_{H\alpha H\beta}$ coupling constants (Supporting Information). These orientations allowed a close spatial proximity between D-Phe^2/Dsa-N^3, and D-Trp^8/Lys^9 side chains; moreover, the tyrosyl group of the residue 10 points toward the Lys^9 side chain. In contrast, the Phe^7 side chain showed almost free rotation about χ_1 angle. Also, the Bzl group of residue 10 was highly flexible.

NMR Analysis of 11. Compound **11** is the chemical precursor of **14**, with an unsaturated CH=CH bridge replacing the disulfide group of **1** (Scheme 2). The coupling constant value ($^3J_{CH=CH}$ = 15.1 Hz) between the two olefinic protons of the bridge and NOE contacts between the same olefinic H_βs of residue 14 (3) established the *E*-geometry about the double bond. No signal attributable to the *Z*-isomer could be detected in the spectra, indicating a unique configurational structure. Compound **11** shows spectral features resembling those found for **14**, with the exception of those of dhDsa-N^3 and dhDsa-C^{14} residues, which obviously feel the effect of the double bond in the side chains. The 3D structures of **11** were calculated as described above. The quality of the structure is reflected by the small rmsd (backbone heavy atoms rmsd = 0.40 Å), which can also be visually depicted from Figure 3d, showing the bundle of 10 conformers representing the 3D structure. A β-turn about residues D-Trp^8-Lys^9, followed by a short 3_{10}-helix along residues Tyr(Bzl)^{10}-Dsa-C^{14}-Thr(ol)^{15} were the main backbone features. An overall enhancement of the backbone conformational rigidity is observed for **11** compared to **14** (backbone rmsd = 0.40 Å vs 0.48 Å). Reduced entities of the NOE violations for the proton couples H_α-9/NH-10, H_α-10/NH-14, and H_α-14/NH-15 (about 0.3 Å), and lower values of the temperature coefficients observed for NH-14 and NH-15 (Supporting Information), compared to the corresponding **14**, indicate that the conformational equilibrium between the extended and the helical structures is shifted toward the helical conformation in **11**. Finally, the side-chain orientations of **11** were also similar to those shown by **14** apart from the Tyr(Bzl)^{10} side chain, which is more flexible in **11**, showing an equilibrium between *trans* and *gauche*$^-$ orientations (Figure 3d).

Conformation-Affinity Relationships and Pharmacophore Model for sst$_5$-Selective Analogues. On the basis of the discussed results, we can draw some conformation−affinity relationships concerning the binding to the sst receptors. As most of the bioactive analogues of SRIF are reported so far,[46] the structures of the peptidomimetics presented here have a β-turn of type II′ (Figures 3a−d) about residues D-Trp^8 and Lys^9. The side chain of D-Trp^8 is in the *trans*-conformer, and the side chain of Lys^9 is in the *gauche*$^-$ conformer, bringing the two side chains adjacent to each other in close proximity. In compounds **2** and **13**, which retain affinity toward sst$_2$, the turn motif is part of a β-hairpin structure. This conformation is very similar to that observed for **1** (Figure 4). A detailed comparison of the structures of **13** (and **2**) with **1** shows a different spatial orientation of the D-Phe^2 aromatic cycle. Because, according to Grace et al.,[47] this moiety belongs to the consensus structural motif of sst$_2$-selective analogues, the different orientation observed for D-Phe^2 aromatic cycle could explain the reduced affinities of **2** and **13** toward sst$_2$ compared to the parent **1**. On this point, a direct involvement of the disulfide bridge in the interaction with the sst$_2$ has also been demonstrated.[45,48] In fact, a disulfide can replace an aromatic moiety in key sst–ligand interactions.[48]

As for **1**, a dynamical equilibrium between β-sheet and helical conformations was observed at the C-terminal residues of analogues **2** and **13**. The increased helical character observed in compound **2** compared to **13** parallels its increased affinity toward sst$_5$ receptor. Actually, Grace et al. have reported that **1** analogues should prefer the helical conformation to fit the sst$_5$

pharmacophore.[47] Accordingly, analogues **11** and **14**, which show high affinity and selectivity toward sst_5, feature a stable helical structure at the C-terminus. In these analogues, the β-turn motif is followed by a short 3_{10}-helix along residues Tyr(Bzl)^{10}-Dsa-C^{14}-Thr(ol)^{15}. The side chain of Tyr(Bzl)^{10}, which apparently stabilizes the helical structure, is in the *gauche*$^-$ conformer and is located in close proximity to the D-Trp^8-Lys^9 pair (Figure 3c,d). If this structure corresponds to the bound conformation of the analogue **14** (and **11**), then the Tyr(Bzl) bulky side chain must accommodate in a suitable hydrophobic pocket within the sst_5 binding site. To explain sst_5 selectivity of analogues **11** and **14**, it can be hypothesized that this side chain is hardly accommodated into the sst_{1-4} binding sites. Nonetheless, the Tyr(Bzl) residue replaced the Thr^{10} in other SRIF analogues showing high-affinity binding toward all the sst receptors.[26] Hence, the selectivity of the new analogues **11** and **14** toward sst_5 should depend on the conformationally restricted helical structure that they adopt. Finally, considering our sst_5-selective analogues, the increased Tyr(Bzl) side chain, flexibly observed in **11** compared to **14**, can account for the reduced affinity toward the sst_5 observed in the first one.

Based on the results reported above, we propose a pharmacophore model for sst_5-selective analogues. The model involves the classical four side chains of the $sst_{2/3/5}$ pharmacophore,[45] namely, those of residues D-Phe^2, Phe^7, D-Trp^8, and Lys^9, plus the Tyr(Bzl)^{10} side chain, which enhanced sst_5 affinity for both compounds **11** and **14**. The distances between the Cγ atoms of these side chains are reported in Table 4. Because **14** is the most potent sst_5 ligand among the analyzed peptides, the relevant distances reported in Table 4 can be proposed as sst_5 pharmacophoric distances. In the same table we also report the Cγ−Cγ distances found by Melacini et al. for the $sst_{2/3/5}$-selective SRIF analogues.[45] It can be observed that the distances found for **14** (and **11**) agree with the $sst_{2/3/5}$ pharmacophore. Recently, the groups of J. Rivier and J. C. Reubi proposed pharmacophore models for sst_1-,[49] sst_2-,[47] sst_3-,[50] and sst_4-selective[51] analogues, by examining the NMR behavior of a large number of cyclic peptides containing the disulfide bridge. To the best of our knowledge, a model of the sst_5 pharmacophore has never been proposed so far.

Conclusions

We have prepared five biostable SRIF analogues with a dicarba moiety replacing the disulfide bridge of the parent **1**. These analogues were prepared by on-resin RCM of allylglycine-containing linear hepta-peptides throughout a new and more efficient synthetic route. First- and second-generation Grubbs catalyst efficiencies were compared. All the analogues were tested for their affinity toward the sst_{1-5} receptor subtypes. Two of them showed moderately high affinity and selectivity for the sst_5 receptor. 3D structures of the active analogues have been determined by ^{1}H NMR spectroscopy. Conformation−affinity relationships indicate that helical propensity well correlates with the peptide−sst_5 affinity. A new pharmacophore model for sst_5 was developed. The proposed pharmacophore model will play an important role in designing highly selective peptide as well as nonpeptide ligands at the sst_5 receptor.

Experimental Section

General Procedures. Fmoc-protected amino acids were purchased from Calbiochem-Novabiochem (Laufelfingen, Switzerland). First- and second-generation Grubbs catalyst and Wilkinson's catalyst were obtained from Aldrich. Fmoc-Hag and Fmoc-O-Bzl-L-tyrosine and $Pd(OH)_2/C$ were purchased from Fluka. H-L-Thr(*t*-Bu)-ol-2-chlorotrityl resin was purchased from Iris Biotech (Marktredwitz, Germany). HATU was obtained from Advanced Biotech Italia (Milan, Italy). Peptide grade DMF was from Scharlau (Barcellona, Spain). All the other solvents and reagents used for SPPS were of analytical quality and used without further purification. Analytical RP-HPLCs were performed on a Beckmann System Gold instrument (model 125S) equipped with a System Gold 166 detector on a Phenomenex Jupiter C18 column (5 μm, 250 × 4.6 mm) using a flow rate of 1 mL/min, with the following solvent system: 0.1% TFA in H_2O (A), 0.1% TFA in MeCN (B)).

Semipreparative RP-HPLC analyses were performed on the same instrument using a flow rate of 4 mL/min with the same solvent system on a Phenomenex Jupiter C18 column (10 μm, 250 × 10 mm). Mass spectra were registered on an ESI LCQ advantage mass spectrometer (Thermo-Finnigan). LC-ESI-MS analyses were performed on a Phenomenex Jupiter C18 column (5 μm, 150 × 2.0 mm) using a flow rate of 200 μL/min on a ThermoFinnigan Surveyor HPLC system coupled to ESI-MS, using the solvent system: H_2O (A), MeCN (B), 1% TFA in H_2O (C). Routine NMR spectra were acquired on a Varian Inova 700 apparatus. DMSO-d_6 was obtained from Aldrich (Milwaukee, U.S.A.). SPPS was performed in Teflon reactor on a manual synthesizer PLS 4 × 4 (AdvancedChemTech).

Synthesis of Linear Peptides 5–7 (Scheme 1). Peptides were synthesized in a Teflon reactor fitted with a polystyrene porous frit. Peptides were prepared using the general Fmoc-SPPS strategy on preswelled H-L-Thr(*t*-Bu)-ol-2-chlorotrityl resin. Couplings were performed by adding 2 equiv of protected amino acid activated by HATU and 4 equiv NMM in DMF, stirring for 45 min for each coupling (Scheme 1) and monitoring by the qualitative ninhydrin (Kaiser) test.[52] At the end of the linear peptides synthesis, a microscale cleavage was performed. Compound **5** and **7** were treated with TFA/H_2O/EDT/phenol (94:2:2:2, 3 h), while compound **6** was treated with TFA/H_2O/EDT/phenol (70:26:2:2, 2.30 h). The resin was filtered off, the solutions were concentrated, the peptide was precipitated from Et_2O, centrifuged dissolved in water, and lyophilized. RP-HPLC analysis of the crude products revealed the presence of the linear peptides in approximately 95% purity, without traces of isomers due to amino acid racemization.

Cyclization and Purification Methods (Scheme 2). The resin aliquots containing the peptides **5**–**7** were swollen for 2 h in anhydrous DCM. The vessels were heated to 45 °C and a DCM solution of catalyst **3** (0.5 mol equiv. calculated on the basis of 0.5 mmol/g of peptide) was added.[11,18,53] The suspension was then stirred for 48 h at 45 °C in the case of compounds **5** and **6** and 52 h for compound **7**. The cyclization was also performed with catalyst **6** in the same conditions, stirring for 24 h for compounds **5** and **6**, and 48 h for compound **7**. The resin aliquots were washed with DCM, DMF, and MeOH, then swelled for 45 min at room temperature in DMF. Fmoc-Hag was deprotected (2.5 mL of 20% piperidine in DMF for 5 min, 4 time repeated) and coupled with Fmoc-D-Phe, as described above, affording the on-resin peptides **8**–**10**, which were deprotected and cleaved, as previously described. The solutions were concentrated and treated with Et_2O giving crude dicarba-analogues **2**, **11**, and **12**, which were suspended in water, and the precipitate was centrifuged off. The aqueous solutions of the peptides **2** and **11**, obtained by RCM with **3**, were prepurified by SPE, eluting with an increased percentage of MeOH in H_2O (from 0 to 50%). The fractions containing 0% MeOH (**11**) and 20% MeOH (**2**) were collected, and the solvent was removed under reduced pressure and lyophilized, giving colorless powders. The small amount of **12** obtained by RCM with **3** was not subjected to SPE and was directly purified by RP-HPLC. Differently, among the peptides achieved with the use of catalyst **4**, only **12** needed prepurification by SPE, collecting the fraction eluted with 20% MeOH. Compounds **2**, **11**, and **12** from both methods were then purified by semipreparative RP-HPLC, and the most abundant chromatographic peaks were collected (Table 1). For all the products, HPLC purity was >98%; ESI-MS (**2**, $[M + H]^+$) calcd, 981.10; found, 981.45; (**11**, $[M + H]^+$) calcd, 1133.34; found, 1133.35; (**12**, $[M + H]^+$) calcd, 1027.22; found, 1027.38 (full experimental data are reported in the Supporting Information).

Reduction Methods. Method A (Scheme 3). A total of 10% w/w of 20% $Pd(OH)_2/C$ was added to the pure peptide **2** (*Z*-isomer) and anhydrous MeOH were added to the mixture. The reaction vessel was purged with N_2 and then H_2 was flushed. The suspension was stirred at 30 °C for 24 h, filtered on celite, the solvent was evaporated under reduced pressure and the crude product was lyophilized. Analytical RP-HPLC still revealed the presence of the unsaturated **2** (20% by HPLC). The product was purified by semipreparative RP-HPLC obtaining **13** (35% yield, HPLC purity >98%). ESI-MS $[M + H]^+$ calcd, 983.53; found, 983.44.

Method B (Scheme 3). To **9**, suspended in a solution of 10% anhydrous MeOH in DCM, Wilkinson's catalyst (2.5 mol %) was added.[25] The reaction vessel was pressured with H_2 (60 psi) and left to stand under stirring at 30 °C for 30 h. The resin was repeatedly washed with DCM and DMF, then D-Phe was coupled to the resin-tethered reduced cyclopeptide **9**. The saturated analogue **14** was cleaved from the resin as previously described and purified by semipreparative RP-HPLC, affording pure **14** (13% yield, HPLC purity >98%). ESI-MS $[M + H]^+$ calcd, 1135.35; found, 1135.50.

NMR Spectroscopy. The samples for NMR spectroscopy were prepared by dissolving the appropriate amount of peptides in 0.40 mL of ^1H_2O (pH 5.0) and 0.10 mL of DMSO-d_6, obtaining 2 mM solutions. TSP was used as internal chemical shift standard. The water signal was suppressed by the hard pulse WATERGATE scheme. NMR experiments were recorded on a Varian Inova-Unity 700 MHz at 277.1 K. Complete ^1H NMR chemical shift assignments were effectively achieved for all the analyzed peptides (Supporting Information) according to the Wüthrich procedure[54] via the usual systematic application of DQF-COSY,[55,56] TOCSY,[57] and NOESY[58] experiments recorded in the phase-sensitive mode using the method from States et al.[59]

Typical data block sizes were 2048 addresses in t_2 and 512 equidistant t_1 values. Before Fourier transformation, the time domain data matrices were multiplied by shifted $\sin^2$ functions in both dimensions. A mixing time of 70 ms was used for the TOCSY experiments. NOESY experiments were run, with mixing times in the range of 150–300 ms. The qualitative and quantitative analyses of DQF-COSY, TOCSY, and NOESY spectra were obtained with the support of the XEASY software package.[60] $^3J_{HN\text{-}H\alpha}$ coupling constants were obtained from 1D ^1H NMR and 2D DQF-COSY spectra. $^3J_{H\alpha\text{-}H\beta}$ coupling constants were obtained from 1D ^1H NMR and 2D PE-COSY spectra, with the last performed with a β flip angle of 35°.[61]

Structural Determinations and Computational Modeling. The NOE-based distance restraints were obtained from NOESY spectra collected with a mixing time of 200 ms. The NOE cross peaks were integrated with the XEASY program and were converted into upper distance bounds using the CALIBA program incorporated into the program package DYANA.[42] 50/200 structures were chosen whose interprotonic distances best fitted NOE-derived distances and then were refined through successive steps of restrained and unrestrained energy minimization calculations using the Discover algorithm (Accelrys, San Diego, CA) and the consistent valence force field (CVFF).[62]

The minimization lowered the total energy of the structures; no residue was found in the disallowed region of the Ramachandran plot. The final structures were analyzed using the InsightII program (Accelrys, San Diego, CA). Graphical representation was carried out with the InsightII program (Accelrys, San Diego, CA).

Determination of Somatostatin Receptor Affinity Profiles. CHO-K1 and CCL39 cells stably expressing human sst_1-sst_5 receptors were grown, as described previously.[63] Cell membrane pellets were prepared and receptor autoradiography was done on 20 μm thick pellet sections (mounted on microscope slides), as described in detail previously.[63] For each of the tested compounds, complete displacement experiments were done with the universal SRIF radioligand [^{125}I]-[Leu^8,D-Trp^{22},Tyr^{25}]-SRIF-28 using increasing concentrations of the unlabeled compounds ranging from 0.1 to 1000 nmol/L. SRIF-28 was run in parallel as control using the same increasing concentrations. IC_{50} values were calculated after quantification of the data using a computer-assisted image processing system. Tissue standards containing known amounts of isotopes, cross-calibrated to tissue-equivalent ligand concentrations, were used for quantification.[63]

Acknowledgment. We thank the Italian Ministry of the University and of the Research (MIUR) for the financial support (PRIN 2005). We also acknowledge the Ente Cassa di Risparmio of Florence for funding and for providing a scholarship. We also thank Prof. P. Frediani and Dr. L. Rosi for giving disposal of the apparatus for Wilkinson's reduction.

Supporting Information Available: Analytical data of the synthesized peptides and NMR data of the analyzed peptides. This material is available free of charge via the Internet at http://pubs.acs.org.

References

(1) Burgus, R.; Brazeau, P.; Vale, W. W. Isolation and Determination of the Primary Structure of Somatostatin (a Somatotropin Release Inhibiting Factor) of Bovin Hypothalamic Origin. Advances in Human Growth Hormone Research; U.S. Government Printing Office: Washington, D.C., 1973; 44−158, Publ. No. (NIH) 74-612.
(2) Rivier, J. Somatostatin: Total Solid Phase Synthesis. *J. Am. Chem. Soc.* **1974**, *96*, 2986–2992.
(3) Pradayrol, L.; Joernvall, H.; Mutt, V.; Ribet, A. N-Terminally Extended Somatostatin: The Primary Structure of Somatostatin-28. *FEBS Lett.* **1980**, *109*, 55–58.
(4) Weckbecker, G.; Lewis, I.; Albert, R.; Schmid, H. A.; Hoyer, D.; Bruns, C. Opportunities in Somatostatin Research: Biological, Chemical and Therapeutical Aspects. *Nat. Rev. Drug Discovery* **2003**, *2*, 999–1018.
(5) Janecka, A.; Zubzycka, M.; Janecki, T. Somatostatin Analogs. *J. Pept. Res.* **2001**, *58*, 91–107.
(6) Bauer, W.; Briner, U.; Dopfner, W.; Haller, R.; Huguenin, R.; Marbach, P.; Petcher, T. J.; Pless, J. SMS201–995: A Very Potent and Selective Analogue of Somatostatin with Prolonged Action. *Life Sci.* **1982**, *31*, 1133–1140.
(7) Lamberts, S. W.; Van der Lely, A. J.; Hofland, L. J. New Somatostatin Analogs: Will They Fulfill Old Promises? *Eur. J. Endocrinol.* **2002**, *146*, 701–705.
(8) Deshmukh, M. V.; Voll, G.; Kühlewein, A.; Schmitt, J.; Kessler, H.; Gemmecker, G. NMR Studies Reveal Structural Differences Between the Gallium and Yttrium Complexes of DOTA-D-Phe^1-Tyr3-Octreotide. *J. Med. Chem.* **2005**, *48*, 1506–1514.
(9) Fichna, J.; Janecka, A. Synthesis of Target-Specific Radiolabeled Peptides for Diagnostic Imaging. *Bioconjug. Chem.* **2003**, *14*, 3–17.
(10) Van Binst, G.; Tourwe′, D. Backbone Modifications in Somatostatin Analogues: Relation Between Conformation and Activity. *Pept. Res.* **1992**, *5*, 8–13.
(11) Willliams, R. M.; Liu, J. Asymmetric Synthesis of Differentially Protected 2,7-Diaminosuberic Acid, a Ring-Closure Metathesis Approach. *J. Org. Chem.* **1998**, *63*, 2130–2132.
(12) Veber, D. F.; Strachan, R. G.; Bergstarand, S. J.; Holly, F. W.; Homnick, C. F.; Hirschmann, R. Nonreducible Cyclic Analogues of Somatostatin. *J. Am. Chem. Soc.* **1976**, *98*, 2367–2369.
(13) Nutt, R. F.; Veber, D. F.; Saperstein, R. Synthesis of Nonreducible Bicyclic Analogues of Somatostatin. *J. Am. Chem. Soc.* **1980**, *102*, 6539–6545.
(14) Gazal, S.; Gelerman, G.; Ziv, O.; Karpov, O.; Litman, P.; Bracha, M.; Afargan, M.; Gilon, C. Human Somatostatin Receptor Specificity of Backbone-Cyclic Analogues Containing Novel Sulfur Building Units. *J. Med. Chem.* **2002**, *45*, 1665–1671.
(15) Hornik, V.; Seri-Levy, A.; Gellerman, G.; Gilon, C. Conformationally constrained Backbone Cyclized Somatostatin Analogs. PCT WO 9804583 A1, 1998.
(16) Grubbs, R. H. Olefin Metathesis. *Tetrahedron* **2004**, *60*, 7117–7140.
(17) Connon, S. J.; Blechert, S. Recent Advances in Alkene Metathesis. *Top. Organomet. Chem.* **2004**, *11*, 93–124.
(18) Miller, S. J.; Blackwell, H. E.; Grubbs, R. H. Application of Ring-Closing Metathesis to the Synthesis of Rigidified Amino Acids and Peptides. *J. Am. Chem. Soc.* **1996**, *118*, 9606–9614.
(19) Reichwein, J. F.; Versluis, C.; Liskamp, R. B. Synthesis of Cyclic Peptides by Ring Closing Metathesis. *J. Org. Chem.* **2000**, *65*, 6187–6195.
(20) Stymiest, J. L.; Mitchell, B. F; Wong, S.; Vederas, J. C. Synthesis of Oxytocin Analogues with Replacement of Sulfur by Carbon Gives Potent Antagonists with Increased Stability. *J. Org. Chem.* **2005**, *70*, 7799–7809.
(21) Schmiedeberg, N.; Kessler, H. Reversible Backbone Protection Enables Combinatorial Solid-Phase Ring-Closing Metathesis Reaction (RCM) in Peptides. *Org. Lett.* **2002**, *4*, 59–62.

(22) Blackwell, H. E.; Sadowsky, J. D.; Howard, R. J.; Sampson, J. N.; Chao, J. A.; Steinmetz, W. E.; O'Leary, D. J.; Grubbs, R. H. Ring-Closing Metathesis of Olefinic Peptides: Design Synthesis, and Structural Characterization of Macrocyclic Helical Peptides. *J. Org. Chem.* **2001**, *66*, 5291–5302.
(23) Kaptein, B.; Broxterman, Q. B.; Schoemaker, H. E.; Ruties, F. P. J.; Veerman, J. J. N.; Kamphuis, J.; Peggion, C.; Formaggio, F.; Toniolo, C. Enantiopure Cα-Tetrasubstituted α-Amino Acids. Chemoenzymatic Synthesis and Application to Turn-Forming Peptides. *Tetrahedron* **2001**, *57*, 6567–6577.
(24) Carotenuto, A.; D'Addona, D.; Rivalta, E.; Chelli, M.; Papini, A. M.; Rovero, P.; Ginanneschi, M. Synthesis of a Dicarba-Analogue of Octreotide Keeping the Type II′ β-Turn of the Pharmacophore in Water Solution. *Lett. Org. Chem.* **2005**, *2*, 274–279.
(25) Wheland, A. N.; Elaridi, J.; Mulder, R. J.; Smith, S. V.; Robinson, A. J; Jackson, W. R. Metal-Catalyzed Tandem Metathesis-Hydrogenation Reactions for the Synthesis of Cyclic Peptides. *Can. J. Chem.* **2005**, *83*, 875–881.
(26) Lewis, I.; Bauer, W.; Albert, R.; Chandramouli, N.; Pless, J.; Weckbecker, G.; Bruns, C. A Novel Somatostatin Mimic with Broad Somatotropine Release Inhibitory Factor Receptor Binding and Superior Therapeutic Potential. *J. Med. Chem.* **2003**, *46*, 2334–2344.
(27) Hsieh, H. P.; Wu, Y. T; Chen, S. T; Wang, K. T. Direct Solid-Phase synthesis of Octreotide Conjugates: Precursors for Use as Tumor-Targeted Radiopharmaceuticals. *Bioorg. Med. Chem.* **1999**, *7*, 1797–1803.
(28) Harris, P. W. R.; Brimble, M. A.; Gluckman, P. D. Synthesis of Cyclic Proline-Containing Peptides via Ring-Closing Metathesis. *Org. Lett.* **2003**, *5*, 1847–1850.
(29) Scholl, M.; Ding, S.; Lee, C. W.; Grubbs, R. H. Synthesis and Activity of a New Generation of Ruthenium-Based Olefin Metathesis Catalysts Coordinated with 1,3-Dimesityl-4,5-dihydroimidazol-2-ylidene Ligands. *Org. Lett.* **1999**, *1*, 953–956.
(30) Morgan, J. P.; Grubbs, R. H. In Situ Preparation of a Highly Active N-Heterocyclic Carbene-Coordinated Olefin Metathesis Catalyst. *Org. Lett.* **2000**, *2*, 3153–5155.
(31) Stimyest, J. L.; Mitchell, B. F.; Wong, S.; Vederas, J. C. Synthesis of Biologically Active Dicarba Analogues of the Peptide Hormone Oxytocin Using Ring-Closing Metathesis. *Org. Lett.* **2003**, *5*, 47–49.
(32) Heather, D. M.; Grubbs, R. H. Purification Technique for the Removal of Ruthenium from Olefin Metathesis Reaction Products. *Tetrahedron Lett.* **1999**, *40*, 4137–4141.
(33) Paquette, L. A.; Schloss, J. D.; Efremov, I.; Fabris, F.; Gallou, F.; Méndez-Andino, J.; Yang, J. A Convenient Method for Removing all Highly-Colored Byproducts Generated During Olefin Metathesis Reaction. *Org. Lett.* **2000**, *2*, 1259–1261.
(34) Jourdant, A.; Gonzalez-Zamora, E.; Zhu, J. Wilkinson's Catalyst Catalyzed Selective Hydrogenation of Olefin in Presence of Aromatic Nitro Function: A Remarkable Solvent Effect. *J. Org. Chem.* **2002**, *67*, 3163–3164.
(35) Burgess, K.; Van der Donk, W. A. In *Encyclopedia of Reagent for Organic Synthesis*; Paquette L. A., Ed.; Wiley: New York, 1995; Vol *2*, pp 1253–1261.
(36) Gilon, C.; Huenges, M.; Mathä, B.; Gellerman, G.; Hornik, V.; Afargan, M.; Amitay, O.; Ziv, O.; Feller, E.; Gamliel, A.; Shohat, D.; Wanger, M.; Arad, O.; Kessler, H. A Backbone-Cyclic, Receptor 5-Selective Somatostatin Analogue: Synthesis, Bioactivity, and Nuclear Magnetic Resonance Conformational Analysis. *J. Med. Chem.* **1998**, *41*, 919–929.
(37) Rohrer, S. P.; Birzin, E. T.; Mosley, R. T.; Berk, S. C.; Hutchins, S. M.; Shen, D. M.; Xiong, Y. S.; Hayes, E. C.; Parmar, R. M.; Foor, F.; Mitra, S. W.; Degrado, S. J.; Shu, M.; Klopp, J. M.; Cai, S. J.; Blake, A.; Chan, W. W. S.; Pasternak, A.; Yang, L. H.; Patchett, A. A.; Smith, R. G.; Chapman, K. T.; Schaeffer, J. M. Rapid Identification of Subtype-Selective Agonists of the Somatostatin Receptor Through Combinatorial Chemistry. *Science* **1998**, *282*, 737–740.
(38) Souers, A. J.; Virgilio, A. A.; Rosenquist, A.; Fenuik, W.; Ellman, J. A. Identification of a Potent Heterocyclic Ligand to Somatostatin Receptor Subtype 5 by the Synthesis and Screening of Beta-Turn Mimetic Libraries. *J. Am. Chem. Soc.* **1999**, *121*, 1817–1825.
(39) Feytens, D.; Cescato, R.; Reubi, J. C.; Tourwe, D. New sst4/5-Selective Somatostatin Peptidomimetics Based on a Constrained Tryptophan Scaffold. *J. Med. Chem.* **2007**, *50*, 3397–3401.
(40) Arison, B. H.; Hirschmann, R.; Veber, D. F. Inferences About the Conformation of Somatostatin at a Biologic Receptor Based on NMR Studies. *Bioorg. Chem.* **1978**, *7*, 447–451.
(41) Wynants, C.; Van Blist, G.; Loosli, H. R. SMS 201–995, an Octapeptide Somatostatin Analogue. *Int. J. Pept. Prot. Res.* **1985**, *25*, 615–621.
(42) Güntert, P.; Mumenthaler, C.; Wüthrich, K. Torsion Angle Dynamics for NMR Structure Calculation with the New Program DYANA. *J. Mol. Biol.* **1997**, *273*, 283–298.
(43) Hutchinson, E. G.; Thornton, J. M. PROMOTIF—A Program to Identify and Analyze Structural Motifs in Proteins. *Protein Sci.* **1996**, *5*, 212–220.
(44) Melacini, G.; Zhu, Q.; Goodman, M. Multiconformational NMR Analysis of Sandostatin (Octreotide): Equilibrium between β-Sheet and Partially Helical Structures. *Biochemistry* **1997**, *36*, 1233–1241.
(45) Melacini, G.; Zhu, Q.; Osapay, G.; Goodman, M. A. Refined Model for the Somatostatin Pharmacophore: Conformational Analysis of Lanthionine-Sandostatin Analogs. *J. Med. Chem.* **1997**, *40*, 2252–2258.
(46) Tyndall, J. D. A.; Pfeiffer, B.; Abbenante, G.; Fairlie, D. P. Over One Hundred Peptide-Activated G Protein-Coupled Receptors Recognize Ligands with Turn Structure. *Chem. Rev.* **2005**, *105*, 793–826.
(47) Grace, C. R. R.; Erchegyi, J.; Koerber, S. C.; Reubi, J. C.; Rivier, J. E.; Riek, R. Novel sst_2-Selective Somatostatin Agonists. Three-Dimensional Consensus Structure by NMR. *J. Med. Chem.* **2006**, *49*, 4487–4496.
(48) Brady, S. F.; Paleveda, W. J.; Arison, B. H.; Saperstein, R.; Brady, E. J.; Raynor, K.; Reisine, T.; Veber, D. F.; Freidinger, R. M. Approaches to Peptidomimetics which Serve as Surrogates for the *cis* Amide Bond: Novel Disulfide-Constrained Bicyclic Hexapeptide Analogs of Somatostatin. *Tetrahedron* **1993**, *49*, 3449–3466.
(49) Grace, C. R. R.; Durrer, L.; Koerber, S. C.; Erchegyi, J.; Reubi, J. C.; Rivier, J. E.; Riek, R. Somatostatin Receptor 1 Selective Analogues. 4. Three-Dimensional Consensus Structure by NMR. *J. Med. Chem.* **2005**, *48*, 523–523.
(50) Gairì, M.; Saiz, P.; Madurga, S.; Roig, X.; Erchegyi, J.; Koerber, S. C.; Reubi, J. C.; Rivier, J. E.; Giralt, E. Conformational Analysis of a Potent SSTR3-Selective Somatostatin Analogue by NMR in Water Solution. *J. Pept. Sci.* **2006**, *12*, 82–91.
(51) Grace, C. R. R.; Koerber, S. C.; Erchegyi, J.; Reubi, J. C.; Rivier, J.; Riek, R. Novel sst4-Selective Somatostatin (SRIF) Agonists. 4. Three-Dimensional Consensus Structure by NMR. *J. Med. Chem.* **2003**, *46*, 5606–5618.
(52) Stewart, J. M.; Young, J. D. In *Solid Phase Peptide Synthesis*, 2nd ed.; Pierce Chemical Company: Rockford, IL, 1984.
(53) Gao, Y.; Lane-Bell, P.; Vederas, J. C. Stereoselective Synthesis of meso-2,6-Diaminopimelic Acid and Its Selectively Protected Derivatives. *J. Org. Chem.* **1998**, *63*, 2133–2143.
(54) Wüthrich, K. *NMR of Proteins and Nucleic Acids*; John Wiley & Sons, Inc.: New York, 1986.
(55) Piantini, U.; Sørensen, O. W.; Ernst, R. R. Multiple Quantum Filters for Elucidating NMR Coupling Network. *J. Am. Chem. Soc.* **1982**, *104*, 6800–6801.
(56) Marion, D.; Wüthrich, K. Application of Phase Sensitive Two-Dimensional Correlated Spectroscopy (COSY) for Measurements of $^1H-^1H$ Spin-Spin Coupling Constants in Proteins. *Biochem. Biophys. Res. Commun.* **1983**, *113*, 967–974.
(57) Braunschweiler, L.; Ernst, R. R. Coherence Transfer by Isotropic Mixing: Application to Proton Correlation Spectroscopy. *J. Magn. Reson.* **1983**, *53*, 521–528.
(58) Jenner, J.; Meier, B. H.; Bachman, P.; Ernst, R. R. Investigation of Exchange Processes by Two-Dimensional NMR Spectroscopy. *J. Chem. Phys.* **1979**, *71*, 4546–4553.
(59) States, D. J.; Haberkorn, R. A.; Ruben, D. J. A Two-Dimensional Nuclear Overhauser Experiment with Pure Absorption Phase Four Quadrants. *J. Magn. Reson.* **1982**, *48*, 286–292.
(60) Bartels, C.; Xia, T.; Billeter, M.; Güntert, P.; Wüthrich, K. The Program XEASY for Computer-Supported NMR Spectral Analysis of Biological Macromolecules. *J. Biomol. NMR* **1995**, *6*, 1–10.
(61) Mueller, L. P. E. COSY, a Simple Alternative to E. COSY. *J. Magn. Reson.* **1987**, *72*, 191–196.
(62) Maple, J.; Dinur, U.; Hagler, A. T. Derivation of Force Fields for Molecular Mechanics and Dynamics from Ab Initio Energy Surface. *Proc. Natl. Acad. Sci. U.S.A.* **1988**, *85*, 5350–5354.
(63) Reubi, J. C.; Schar, J. C.; Waser, B.; Wenger, S.; Heppeler, A.; Schmitt, J. S.; Macke, H. R. Affinity Profiles for Human Somatostatin Receptor Subtypes SST1-SST5 of Somatostatin Radiotracers Selected for Scintigraphic and Radiotherapeutic Use. *Eur. J. Nucl. Med.* **2000**, *27*, 273–282.

JM070886I